Electronic Supplementary Information

Experimental Section

Materials: Nickel nitrate hexahydrate ($Ni(NO_3)_2 \cdot 6H_2O$), iron (III) nitrate nonahydrate ($Fe(NO_3)_3 \cdot 9H_2O$), sodium sulfide nonahydrate ($Na_2S \cdot 9H_2O$), ammonium fluoride (NH_4F), urea, ruthenium oxide (RuO_2), Pt/C (20 wt% Pt on Vulcan XC-72R), Nafion (5 wt%), hydrochloric acid (HCl), ethylalcohol (C_2H_5OH), sodium chloride (NaCl), potassium hydroxide (KOH), and sodium carbonate (Na_2CO_3) were obtained from Aladdin Industrial Co. Natural seawater was collected from Weihai, Shandong, China, and most of the magnesium and calcium salts were removed by first adding 3.4 g Na_2CO_3 to 500 mL of natural seawater before use. All the reagents were used as received without further purification. Ni foam (NF) was obtained from Shenzhen Green and Creative Environmental Science and Technology Co. Ltd. The water used throughout all experiments was purified through a Millipore system.

Preparation of NiFe-LDH/NF and NiFeS/NF: Firstly, a well-cut small piece of NF (2.0 × 3.0 cm^2) was sonicated in HCl, ethanol, and distilled water, respectively. The pre-treated NF was put into a solution containing 40 mL deionized water, 0.582 g $Ni(NO_3)_2 \cdot 6H_2O$, 0.404 g $Fe(NO_3)_3 \cdot 9H_2O$, 0.148 g NH_4F, and 0.6 g urea in a Teflon-lined autoclave and heated at 120 °C for 6 h to obtain NiFe-LDH/NF. It was washed with deionized water and ethanol several times, and dried at 60 °C. Then the synthetic sample was immersed in 0.2 M $Na_2S \cdot 9H_2O$ solution in a Teflon-lined autoclave for the hydrothermal treatment (100 °C, 8 h). After the autoclave was cooled down naturally to room temperature, the sample was moved out, washed with deionized water and ethanol several times and dried at 60 °C for 30 min. Finally, NiFeS/NF was obtained.

Preparation of RuO_2 or Pt/C on NF: 5 mg RuO_2 (or 20% Pt/C) was added in a solution containing 30 μL of Nafion, 485 μL of ethanol, and 485 μL of deionized water with the aid of ultrasonication (30 min) to form a homogeneous ink (5 mg mL^{-1}). 280 μL of catalyst ink was dropped onto a piece of cleaned NF (1.0 × 0.5 cm^2)

with a loading mass of 1.4 mg.

Characterization: XRD data was acquired from a LabX XRD-6100 X-ray diffractometer with a Cu Kα radiation (40 kV, 30 mA) of wavelength of 0.154 nm (SHIMADZU, Japan). SEM images were collected on a GeminiSEM 300 scanning electron microscope (ZEISS, Germany) at an accelerating voltage of 5 kV. TEM images were acquired on a HITACHI H-8100 electron microscope (Hitachi, Tokyo, Japan) operated at 200 kV. XPS measurements were performed on an ESCALABMK II X-ray photoelectron spectrometer using Mg as the exciting source. In-situ Raman spectroscopy was recorded on the Horiba-Xplora Plus confocal microscope with 532 nm laser in ~20 mL of 0.1 M KOH + Seawater.

Electrochemical measurements: Electrochemical OER and HER experiments were performed with the CHI 760E electrochemical workstation, using the prepared samples (1 × 0.5 cm^2), carbon rod, and Hg/HgO as the working electrode, counter electrode, and reference electrode, respectively. The water-splitting performance of the electrolyzers were tested in a two-electrode system, where OER electrodes are as the anode and HER electrodes as the cathode. Three different electrolytes, including 1 M KOH, 1 M KOH + 0.5 M NaCl, and 1 M KOH + Seawater, were used, and the pH was about 14.0. All measured potentials were referenced to that of reversible hydrogen electrode (RHE) ($E_{RHE} = E_{Hg/HgO} + 0.059 \times pH + 0.098$ V). Electrochemical impedance spectroscopy (EIS) measurements were performed at open circuit potentials between 110 to 0.01 Hz with an amplitude of 5 mV. The catalytic activity of catalysts was determined by linear sweep voltammetry (LSV) curves with a scan rate of 5 mV s^{-1}. The double-layer capacitance (C_{dl}) values were obtained via cyclic voltammetry (CV) curves with the scan rates of 10−100 mV s^{-1}. All data (except for Fig. S5) have been reported with iR compensation. The iR-compensated potential was obtained after the correction of solution resistance measured following the equation: $E_{corr} = E - iR$, where E is the original potential, R is the solution resistance, i is the corresponding current, and E_{corr} is the iR-compensated potential.

DFT calculation: First-principles calculations with spin-polarized were carried out

based on density functional theory (DFT) implemented in the VASP package,[1] and the interaction between valence electrons and ionic core were expanded using the projector augmented wave (PAW)[2] approach with a cutoff of 400 eV. Perdew-Burke-Ernzerhof functional (PBE) with semi-empirical corrections of DFT-D3 was adopted to describe exchange-correlation functional effect[3] based on general gradient approximation (GGA). $FeNi_2S_4$ (311) Slab model was constructed with a vacuum layer of 10 Å in the z direction to avoid the interaction between layers. The force convergence thresholds are 0.02 eV/Å and the total energy less than $1E^{-5}$ eV, respectively. The theoretical calculation results were processing and analyzed by VASPKIT software.[4]

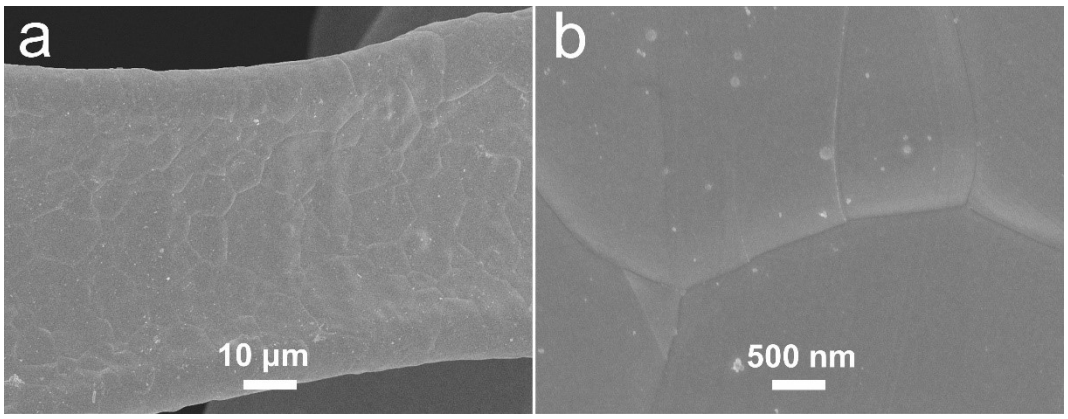

Fig. S1. (a) Low- and (b) high-magnification SEM images of bare NF.

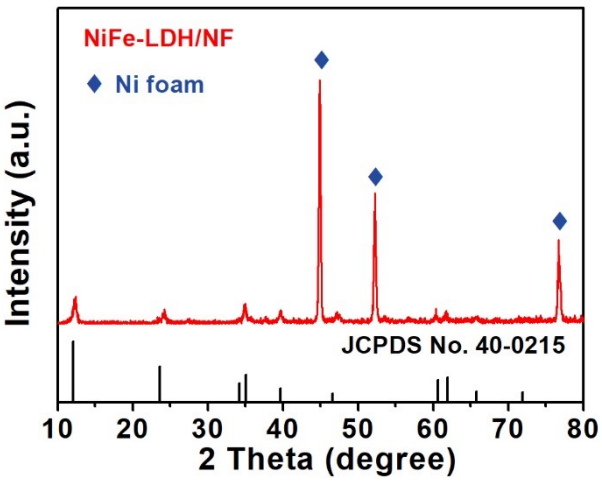

Fig. S2. XRD pattern of NiFe-LDH/NF.

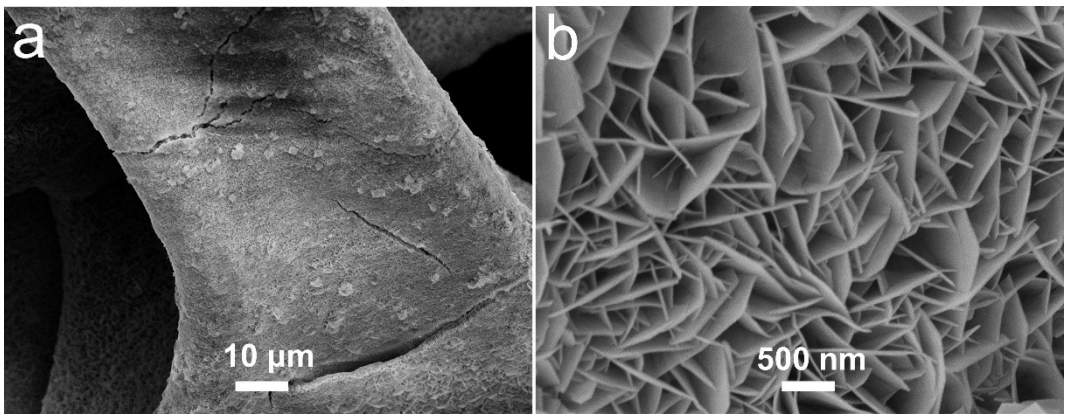

Fig. S3. (a) Low- and (b) high-magnification SEM images of NiFe-LDH/NF.

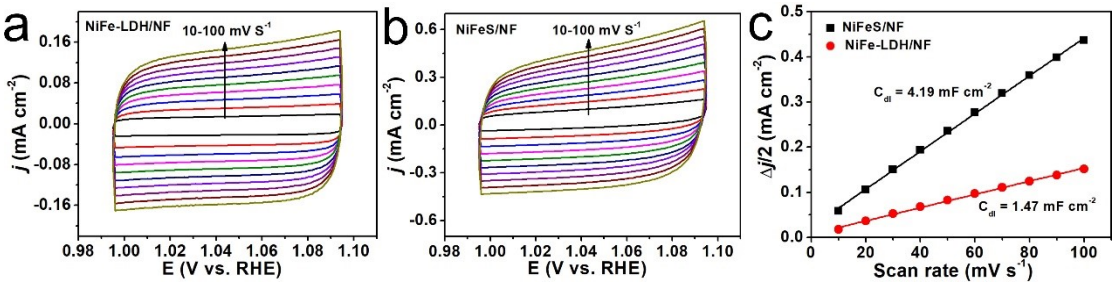

Fig. S4. CV curves of (a) NiFe-LDH/NF and (b) NiFeS/NF. (c) Double-layer capacitance (C_{dl}) plots of NiFe-LDH/NF and NiFeS/NF samples.

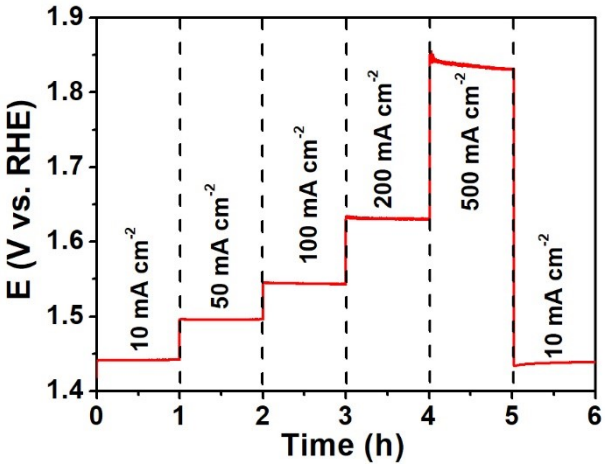

Fig. S5. Multi-current process of NiFeS/NF. The current density started at 10 mA cm^{-2} and ended at 10 mA cm^{-2} without iR correction.

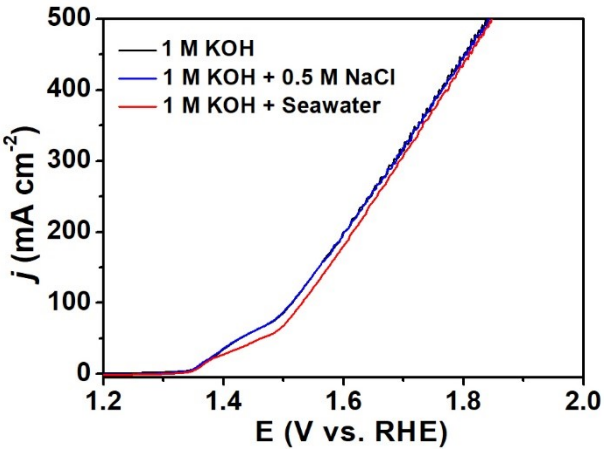

Fig. S6. LSV curves of NiFeS/NF without iR compensation for OER in different electrolytes.

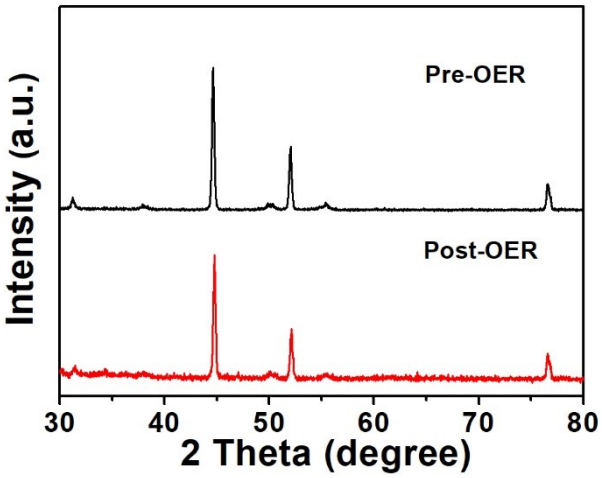

Fig. S7. XRD patterns for pre- and post-OER NiFeS/NF tested in 1 M KOH + Seawater electrolyte.

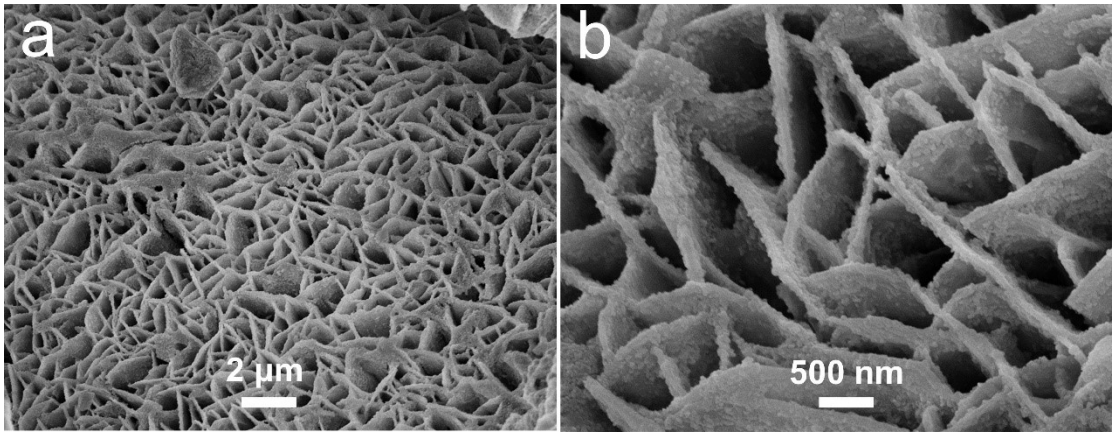

Fig. S8. (a) Low- and (b) high-magnification SEM images of post-OER NiFeS/NF tested in 1 M KOH + Seawater electrolyte.

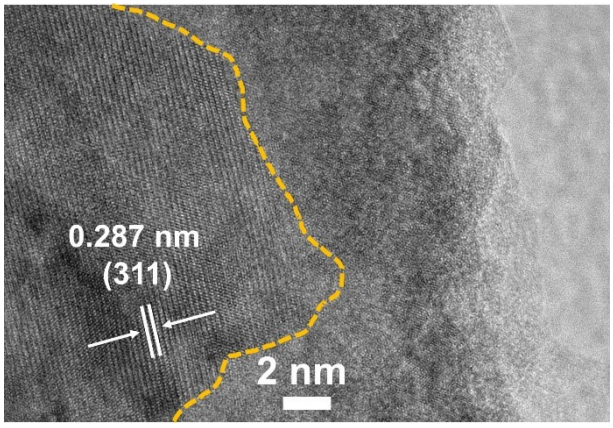

Fig. S9. HRTEM image of NiFeS after post-OER tested in 1 M KOH + Seawater electrolyte.

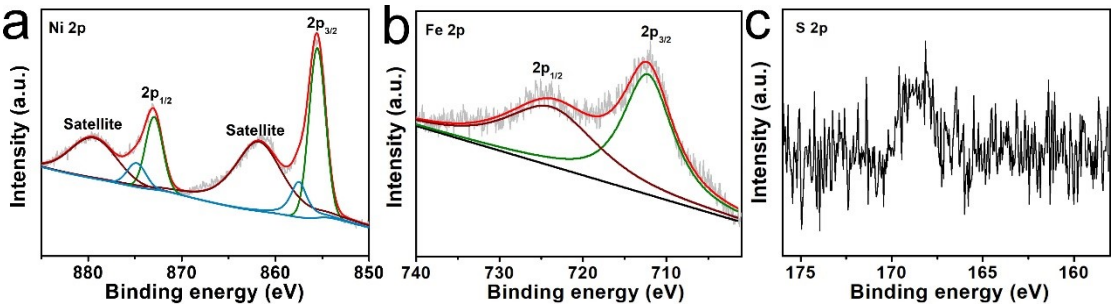

Fig. S10. High-resolution XPS spectra for post-OER NiFeS tested in 1 M KOH + Seawater electrolyte in the (a) Ni 2p, (b) Fe 2p, and (c) S 2s regions.

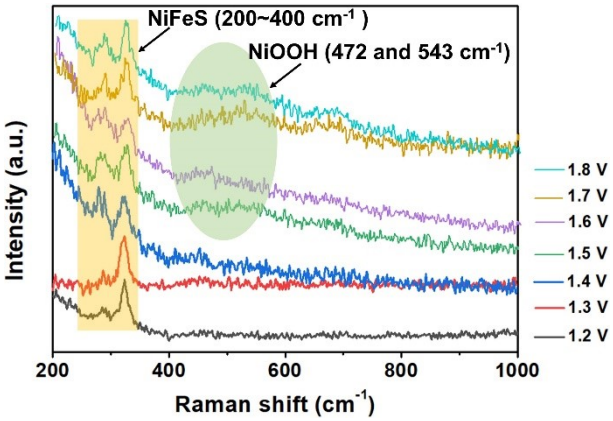

Fig. S11. In-situ potential-dependent Raman spectra of NiFeS electrode in alkaline seawater.

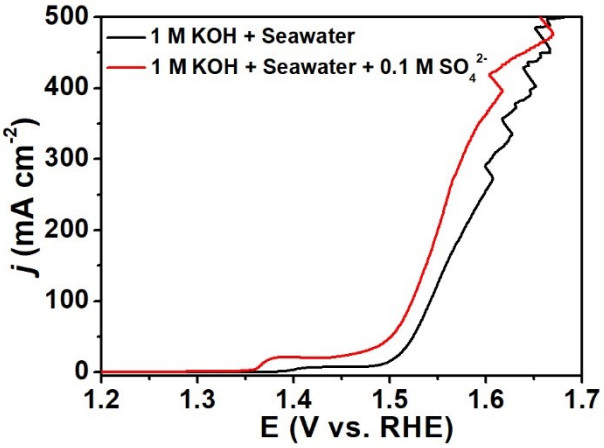

Fig. S12. LSV curves of NiFeS/NF recorded in 1 M KOH + Seawater without and with 0.1 M SO_4^{2-} for OER.

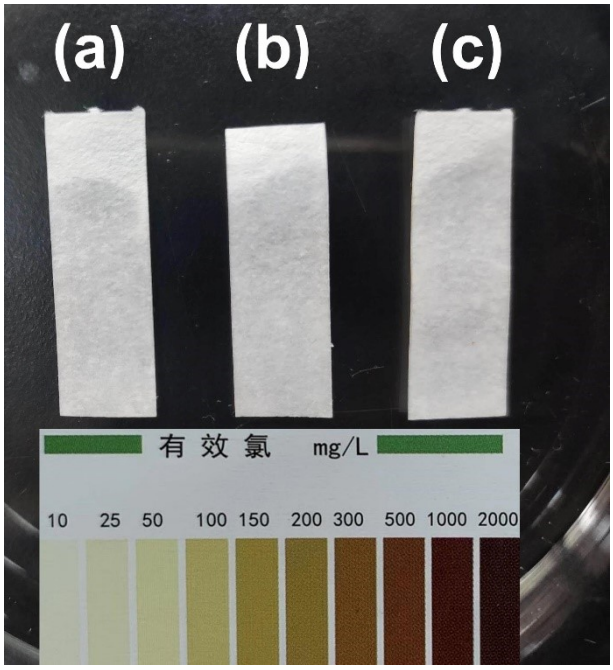

Fig. S13. Photograph of (a) Colorimetric paper tested in 1 M KOH + Seawater before OER stability experiment and colorimetric paper tested in 1 M KOH + Seawater after OER stability experiments at current densities of (b) 100 and (c) 500 mA cm^{-2}.

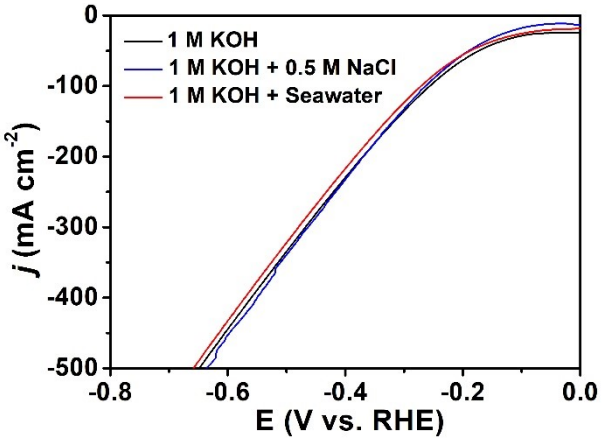

Fig. S14. LSV curves of NiFeS/NF without iR compensation for HER in different electrolytes.

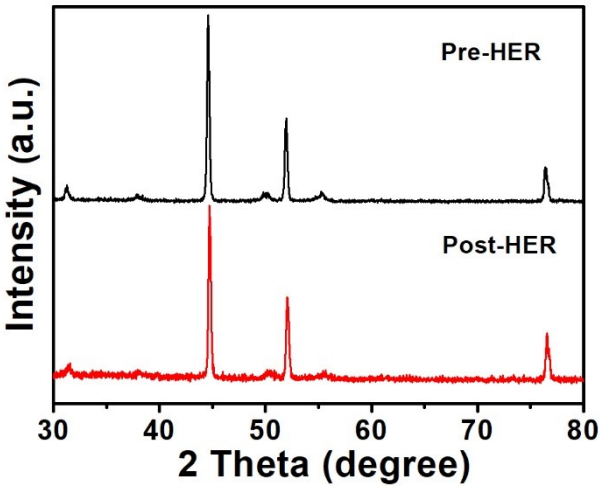

Fig. S15. XRD patterns for pre- and post-HER NiFeS/NF tested in 1 M KOH + Seawater electrolyte.

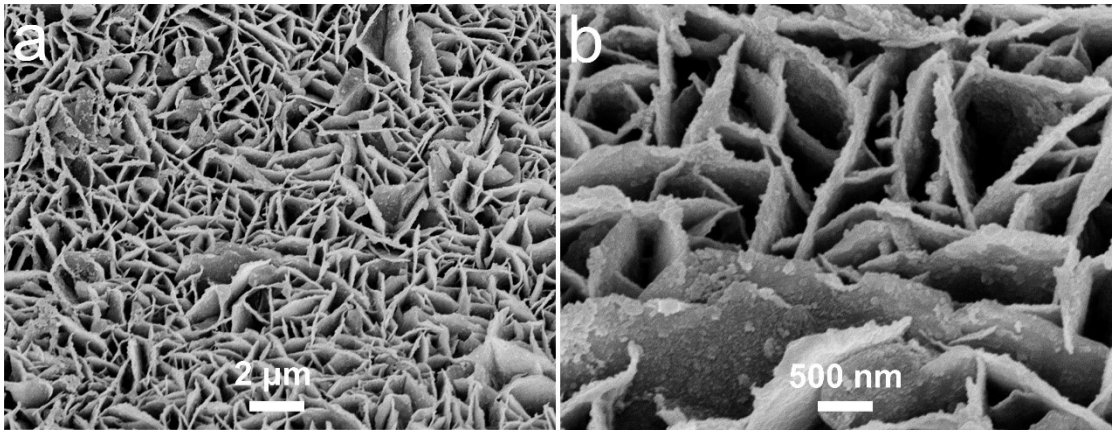

Fig. S16. (a) Low- and (b) high-magnification SEM images of post-HER NiFeS/NF tested in 1 M KOH + Seawater electrolyte.

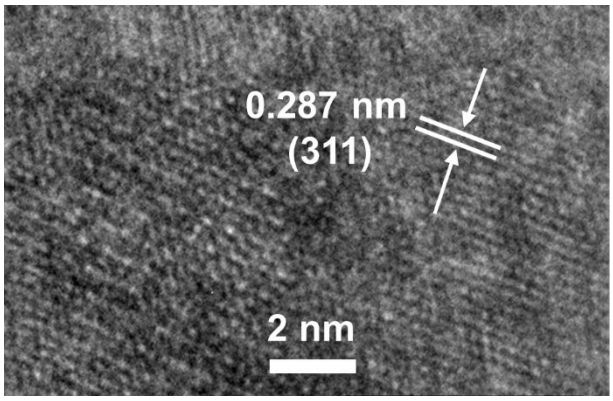

Fig. S17. HRTEM image of post-HER NiFeS tested in 1 M KOH + Seawater electrolyte.

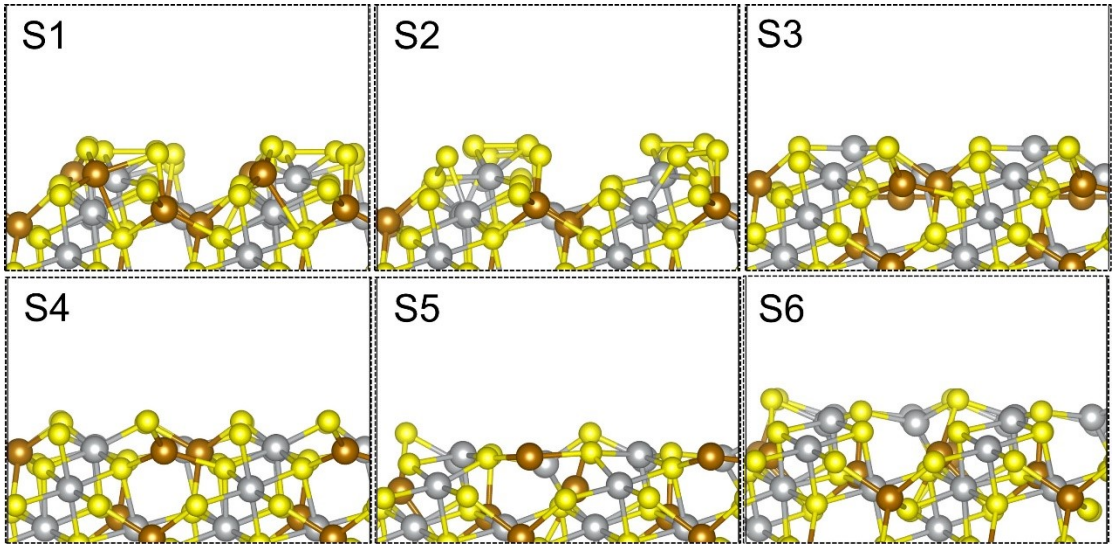

Fig. S18. $FeNi_2S_4$ (311) surface with different terminated face; gray, brown and yellow spheres denote the Ni, Fe, and S.

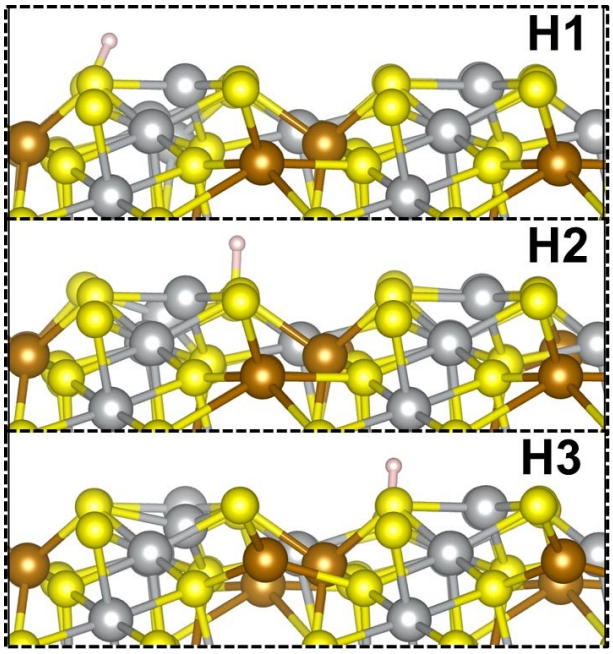

Fig. S19. Atomic configurations; gray, brown and yellow spheres denote the Ni, Fe, and S.

Table S1. The EIS parameters of the samples.

Catalyst	R_{ct}/Ω	R_s/Ω
NiFeS/NF	4.36	1.54
NiFe-LDH/NF	16.70	1.61

Table S2. Comparison of OER performances for NiFeS/NF with other reported OER electrocatalysts.

Electrocatalyst	Electrolyte	Overpotential @ 100 (mV @ mA cm^{-2})	Reference
NiFeS/NF	1 M KOH	215	This Work
	1 M KOH + Seawater	226	
CoP_x@FeOOH/NF	1 M KOH	254	*Appl. Catal., B,* 2021, **294**, 120256
	1 M KOH + Seawater	283	
S-(Ni,Fe)OOH/NF	1 M KOH	281	*Energy Environ. Sci.,* 2020, **13**, 3439–3446
	1 M KOH + Seawater	300	
Mo-CoP_x/NF	1 M KOH	420	*Mater. Today Nano,* 2022, **18**, 100216
	1 M KOH + Seawater	\	
Ni_2P-Fe_2P/NF	1 M KOH	261	*Adv. Funct. Mater.,* 2021, **31**, 2006484
	1 M KOH + Seawater	305	
1D-Cu@Co-CoO/Rh	1 M KOH	380	*Small,* 2021, **17**, 2103826
	1 M KOH + Seawater	400	
NiFe-LDH@$FeNi_2S_4$/NF	1 M KOH	240	*Adv. Funct. Mater.,* 2022, **32**, 2200951
	1 M KOH + Seawater	271	
NiMoN@NiFeN/NF	1 M KOH	277	*Nat. Commun.,* 2019, **10**, 5106
	1 M KOH + Seawater	307	
Mo-Ni_3S_2/NF	1 M KOH	280	*Energy Fuels,* 2022, **36**, 2910–2917
	1 M KOH + Seawater	291	
NiFe/NiS_x/NF	1 M KOH	\	*Proc. Natl Acad. Sci. USA* 2019, **116**, 6624–6629
	1 M KOH + Seawater	350	
BZ-NiFe-LDH/CC	1 M KOH	230	*Nano Res. Energy,* 2022, DOI: 10.26599/NRE.2022.9120028
	1 M KOH + Seawater	300	
N-CDs/NiFeLDH/NF	1 M KOH	260	*Nano Res.,* 2022, **15**, 7063–7070
	1 M KOH + Seawater	340	
NiCoS/NF	1 M KOH	270	*Appl. Catal., B,* 2021, **291**, 120071
	1 M KOH + Seawater	360	
$Ni(OH)_2$-TCNQ/GP	1 M KOH	340	*Nano Res.,* 2022, **15**, 6084–6090
	1 M KOH + Seawater	382	

Table S3. Comparison of HER performances for NiFeS/NF with other reported HER electrocatalysts.

Electrocatalyst	Electrolyte	Overpotential @ –100 (mV @ mA cm^{-2})	Reference
NiFeS/NF	1 M KOH	196	This Work
	1 M KOH + Seawater	217	
CoP_x/NF	1 M KOH	170	*Appl. Catal., B,* 2021, **294**, 120256
	1 M KOH + Seawater	190	
S-$NiMoO_4$@NiFe-LDH/NF	1 M KOH	170	*J. Colloid Interface Sci.,* 2022, **613**, 349–358
	1 M KOH + Seawater	220	
Ni_2P-Fe_2P/NF	1 M KOH	225	*Adv. Funct. Mater.,* 2021, **31**, 2006484
	1 M KOH + Seawater	252	
Co-N, P-HCS	1 M KOH	\	*Adv. Mater.,* 2022, **34**, 2204021
	1 M KOH + Seawater	287	
1D-Cu@Co-CoO/Rh	1 M KOH	280	*Small,* 2021, **17**, 2103826
	1 M KOH + Seawater	320	
Ni-SN@C	1 M KOH	150	*Adv. Mater.,* 2021, **33**, 2007508
	1 M KOH + Seawater	180	
NiMoN/NF	1 M KOH	84	*Nat. Commun.,* 2019, **10**, 5106
	1 M KOH + Seawater	82	
(Co, Fe)PO_4/IF	1 M KOH	210	*Nanomaterials,* 2021, **11**, 2989
	1 M KOH + Seawater	240	
Ni-SA/NC	1 M KOH	245	*Adv. Mater.,* 2021, **33**, 2003846
	1 M KOH + Seawater	255	
$Ru_{1,n}$-$ZnFe_2O_X$-C	1 M KOH	180	*Small*, 2022, **18**, 2204155
	1 M KOH + Seawater	\	
Ru_2P@Ru/CNT	1 M KOH	198	*Chinese J. Catal.,* 2022, **43**, 1148–1155
	1 M KOH + Seawater	128	
Ni/V_2O_3/NF	1 M KOH	139	*Chem. Eng. J.,* 2022, **450**, 138079
	1 M KOH + Seawater	418	

Table S4. Comparison of overall water splitting performance for NiFeS/NF with other reported bifunctional electrocatalysts.

Electrocatalyst	Electrolyte	Voltages @ 100 (V @ mA cm^{-2})	Reference
NiFeS/NF	1 M KOH	1.65	This Work
	1 M KOH + Seawater	1.67	
Ni_3S_2-MoS_2-Ni_3S_2/NF	1 M KOH	1.88	*Electrochimica Acta,* 2021, **390**, 138833
	1 M KOH + Seawater	1.82	
S,P-(Ni,Mo,Fe)OOH/NiMoP	1 M KOH	1.69	*Appl. Catal., B,* 2021, **293**, 120215
	1 M KOH + Seawater	1.74	
Mo-CoP_x/NF	1 M KOH	2.01	*Mater. Today Nano,* 2022, **18**, 100216
	1 M KOH + Seawater	2.16	
Ni_2P-Fe_2P/NF	1 M KOH	1.682	*Adv. Funct. Mater.,* 2021, **31**, 2006484
	1 M KOH + Seawater	1.811	
NiFe-PBA-gel-cal	1 M KOH	1.57	*Adv. Sci.,* 2022, **9**, 2200146
	1 M KOH + Seawater	1.64	
RuNi-Fe_2O_3/IF	1 M KOH	1.66	*Chinese J. Catal*., 2022, **43**, 2202–2211
	1 M KOH + Seawater	1.73	
NiFeP/NF	1 M KOH	1.57	*Appl. Catal., B,* 2022, **302**, 120862
	1 M KOH + Seawater	1.62	
1D-Cu@Co-CoO/Rh	1 M KOH	2.1	*Small,* 2021, **17**, 2103826
	1 M KOH + Seawater	1.9	
NF@$NiMoO_4$/N/P	1 M KOH	1.69	*J. Electrochem. Soc.,* 2022, **169**, 046511
	1 M KOH + Seawater	1.70	
Co-Fe_2P/NF	1 M KOH	\	*Appl. Catal., B,* 2021, **297**, 120386
	1 M KOH + Seawater	1.69	
MoN−Co_2N	1 M KOH	1.63	*ACS Appl. Mater. Interfaces,* 2022, **14**, 41924–41933
	1 M KOH + Seawater	1.70	
S-$NiMoO_4$@NiFe-LDH/NF	1 M KOH	\	*J. Colloid Interface Sci.,* 2022, **613**, 349–358
	1 M KOH + Seawater	1.73	

References

1 G. Kresse and J. Hafner, *Phys. Rev. B,* 1994, **49**, 14251–14269.

2 G. Kresse and D. Joubert, *Phys. Rev. B,* 1999, **59**, 1758–1775.

3 J. P. Perdew, K. Burke, and M. Ernzerhof, *Phys. Rev. Lett.,* 1996, **77**, 3865–3868.

4 V. Wang, N. Xu, J. Liu, G. Tang and W. Geng, *Comput. Phys. Commun.,* 2021, **267**, 108033.